TRANSNAV the International Journal on Marine Navigation and Safety of Sea Transportation
http://www.transnav.eu
Volume 15
Number 2
June 2021
DOI: 10.12716/1001.15.02.24

Estimation of Changes in Marine Traffic Flow Due to Installation of Virtual Buoys Based on the OZT Method

G. Fukuda, H. Tamaru & R. Shoji
Tokyo University of Marine Science and Technology, Tokyo, Japan

ABSTRACT: In this study, changes in maritime traffic flow due to the installation of virtual buoys were analysed from the perspective of collision, based on the obstacle zone by target (OZT) method. The existence of an OZT within ±2° in the bow direction is considered to be dangerous; all the OZTs that a vessel encountered at the time when this orientation prevailed were subjected to analysis. For the calculation of the OZT model, an SD3 model was used. The estimated OZT was used to calculate the OZT density, and the positions of the ships that were encountering the OZT were used for the analysis. It was found that the OZT density at the locations where collisions had occurred in the past was approximately 0.01 [times/km^2]. After the installation of virtual buoys, most places around there were reduced to around approximately 0.005 [times/km^2]. The results imply that the installation of virtual buoys has reduced the risk of collisions. In contrast, the OZT density in the southern region of Buoy 1 increased from approximately 0.005 [times/km^2] to approximately 0.01 [times/km^2], suggesting that a more detailed analysis of this area is required.

1 INTRODUCTION

The Japan Coast Guard consolidated the Tokyo Bay Maritime Traffic Center and the four port traffic control offices (Tokyo, Yokohama, Kawasaki, and Chiba) into the Tokyo Wan Vessel Traffic Service Centre on 31 January 2018 [5]. This is expected to improve both safety and efficiency in Tokyo Bay, which is one of the most congested sea areas in Japan, by eliminating poor traffic service areas where ships are not provided with accurate information, allowing the ships under control to navigate on time without waiting for traffic lights or congestion and allowing ships not under control to navigate seamlessly with the information provided, such that they are not affected by the ships under control. The bay entrance, in the vicinity of the Tsurugisaki-Sunosaki Line and the entrance to the Uraga Suido Traffic Route (Uraga Suido), is known to be accident-prone; collisions have occurred because of the intermingling of vessel traffic. Accordingly, a study on marine traffic control measures at the entrance of Tokyo Bay was conducted [13]. In this study, a questionnaire survey was conducted among the concerned parties regarding the areas where they experienced discomfort. To rectify marine traffic based on virtual automatic identification system (AIS) route signs in this area, the marine traffic flow was simulated, and the status of vessel traffic in the area was determined. Consequently, the necessity of establishing a virtual AIS route sign in the southern part of Uraga Suido and separating the traffic flow of vessels entering and leaving the channel by a line connecting the sign and the lighted Buoy 1 at the centre of Uraga Suido, was realized. The location of the virtual AIS was studied, and the changes in marine traffic flow due to the installation of the virtual AIS were investigated by simulation. Consequently, it was confirmed that the

rectification effect of the installation of the virtual AIS improved the safety. Since 1 March 2019, a new maritime traffic route designation has been established in accordance with the Maritime Traffic Safety Act for the Tokyo Bay entrance sea area [6]. Accordingly, the vessels entering and exiting Uraga Suido are expected to navigate directly between the recommended passage established off the west coast of Izu Oshima and the sea area where the rectification is expected to occur, and the traffic flow of vessels entering and exiting Tokyo Bay is expected to be organised in the sea area between the west coast of the island and Uraga Suido [13]. This is believed to reduce dangerous encounters between vessels, such as the one that actually led to the collision described later in this paper. However, no study has yet been conducted to analyse changes in traffic flow after the installation of virtual buoys, from the perspective of collisions. Therefore, in this study, we investigated the changes in traffic flow by applying the obstacle zone by target (OZT) analysis method, which the authors have been studying for some time now [1–3]. In this study, under the condition that the OZT exists in the range of ±2°, based on the direction of a ship's course, the OZT density and the position of the ship at the time when this orientation prevails, are analysed. By analysing the changes in traffic flow at the past collision sites based on the proposed analysis method, we investigated the trend of the change in marine traffic flow in terms of collision zones.

2 ESTIMATION OF OZT DENSITY AND VESSEL POSITION UNDER THE CONDITION THAT OZT EXISTS IN THE DIRECTION OF HEADING

OZT was estimated based on the safety passing distance (SD) according to the matching relationship with the target vessel [1, 4]. In the OZT density analysis, all OZTs within a set distance range were included in the calculation [1]. However, a problem was encountered because few OZTs did not pose any danger. Therefore, to avoid calculating non-dangerous OZTs, the authors only considered the OZTs appearing in the direction of the ship path for calculation [12]. While calculating the OZTs, it was difficult to estimate which OZTs increased the overall OZT density because the OZTs lengthened, particularly, in the situations where ships were navigating courses that were close and almost similar to that of the test ship. To solve this problem, the authors divided the diameter of the SD into three parts and employed the SD3 method, which was first introduced by Prof. Imazu Hayama in our OZT study group, to calculate the OZT. In addition, a vertical line was drawn from the proximate side of the calculated OZT to the line connecting the farther side of the OZT and the ship, and the intersection point was used as the new OZT. All the methods are described in the following sections.

2.1 *OZT calculation based on SD3 method*

The basic method to determine the OZT is to set the SD in the vicinity of the ship and establish a course that does not allow other ships to enter that area. In this study, we set the SD such that, it is divided into three circles within the conventionally used SD. The method of determining the OZT course by setting the SD in this manner is described as follows.

1. A normal SD is drawn that divides the conventional SD into three equal parts in the direction of the velocity vector of a nearby target ship (hereinafter referred to as "target").
2. Tangent lines are drawn from the position of the target ship to the SD (blue, purple, green, and yellow dashed lines in Figure 1).
3. Each tangent line is parallelised such that it touches the tip of the velocity vector of the target ship, extended from the position of the test ship.
4. The intersections of the parallel tangent lines and the speed circle of the test ship are determined.
5. The range of the line connecting the outermost point of each intersection with the position of the test ship is the range of the OZT course (OZT Co1, OZT Co2, OZT Co3, and OZT Co4 in Figure 1).

The courses on both sides that represent each OZT range are defined as OZT Co1 and OZT Co2 and OZT Co3 and OZT Co4. The vector connecting each OZT Co1, Co2, Co3, and Co4 to the end of the velocity vector of the target ship is the direction and magnitude of relative velocities of the ship as it traverses each course. For example, the direction from the intersection of OZT Co1 and the test ship's velocity circle to the tip of the target ship's velocity vector is the direction of the relative vector when the test ship travels along Course OZT Co1, and its magnitude is the relative velocity. The Time to the Closest Position of Approach (TCPA) when navigating each OZT Co can be obtained by dividing the length of the tangent line drawn from the target ship to each SD by the respective relative velocity.

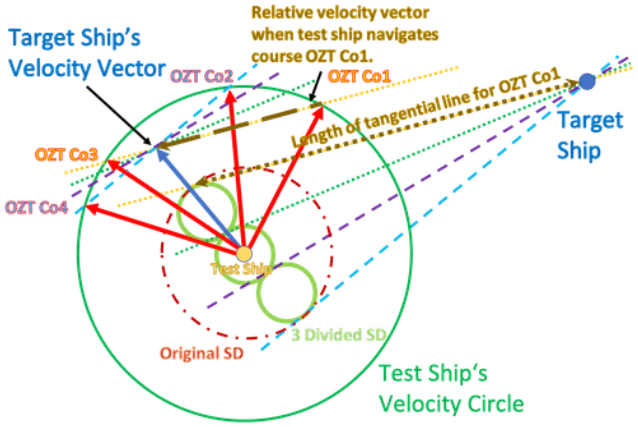

Figure 1. Procedure to determine the OZT Course (Co) by drawing.

It is considered that OZT1 is the endpoint of the OZT closest to the test ship, OZT2 is the endpoint of the OZT on the farther side, the angle of inclination is θ, and the distance from the test ship to OZT1 is D1. Dropping the vertical line from OZT1, the intersection of the line connecting the test ship and OZT2 is OZT2' as shown Figure 2. Hereinafter, the zone connecting OZT1 and OZT2' is referred to as SD3C OZT.

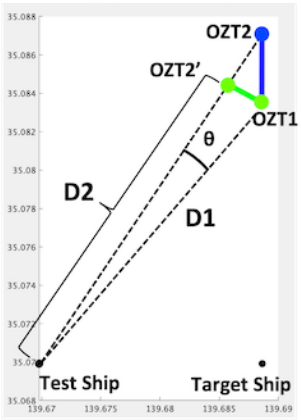

Figure 2. Relationship between OZT1, OZT2, and OZT2'.

The distance, D2, between the test ship and OZT2' is obtained using the following formula:

$$D2 = D1\cos\theta \tag{1}$$

The parameters for the test ship and target ships were set as shown in Table 1. Figure 3 shows the relationship between the conventional OZT, the OZT when SD is divided into three parts (SD3 OZT), and the OZT obtained from the angle of elevation, θ (SD3C OZT), when the course of the target ship is turned every 30° from 0° to 360°. The diameter of the conventional SD was set to 290 m. As can be seen from Figure 3, the SD3C OZT used in this study clearly shows the horizontal range where the target ship cannot proceed when viewed from the perspective of the test ship. However, it should be noted that the SD3C OZT used in this study cannot be used in the evaluation of a case where both ships avoid each other over a short distance.

Table 1. Parameters for test ship and target ship.

	SOG [knot]	Length [m]	Width [m]
Test Ship	10	200	36
Target Ship	7	90	12

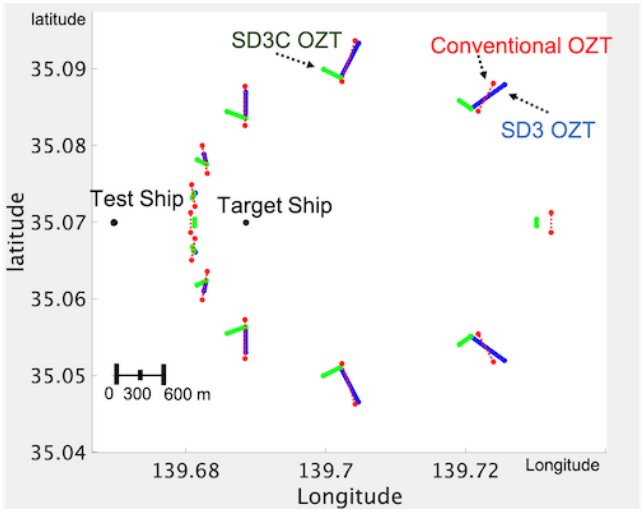

Figure 3. Relationship between Normal OZT, SD3 OZT, and SD3C OZT.

2.2 *Calculation conditions for OZT*

For the existence of an OZT with one of the target ships within ±2° on the test ship's course [12], all the OZTs within ±45° of the test ship's course and within 4 miles, were included in the analysis, as shown in Figure 4. The distance between the ships and the distance to the OZTs were also set within 4 miles. If one endpoint of an OZT was within 4 miles and the other endpoint was set at a point beyond 4 miles, the time to reach the farther OZT was calculated as 30 min. TS stands for "Target Ship". The ship positions in the estimation results (e.g. Figure 9) that appear later show the positional relationship between the test ship and target ships.

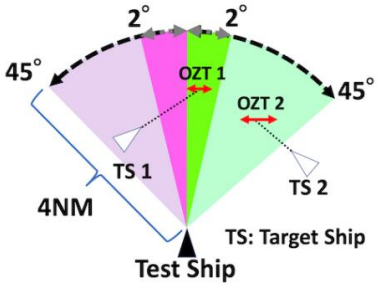

Figure 4. Example of OZT calculation conditions.

2.3 *OZT Density*

The OZT density is the sum of the existence time of the OZTs in the grid divided by the observation time. However, because this study uses data that are interpolated over 30 s, it presents an error of ±30 s. For the navigational density of the test ship, the time that the test ship has existed in the grid can be estimated from the test ship's speed; however, it is difficult to estimate the existence time of the OZT, whose state changes depending on the paths of the target and the test ships. A feasible solution is to use the AIS data interpolated to 1 s [1]; however, it is extremely time-intensive to estimate the existence time, owing to the heavy marine traffic near the entrance of the Tokyo Bay. The OZT density at the time of the OZT encounter is defined as the number of OZTs per unit area, per unit time, in each mesh and is calculated using the following formula:

$$D_{OZT} = \frac{\sum_{i=1}^{n} eOZT_i}{a \cdot T} \tag{2}$$

where:
D_{OZT}: OZT density [times/km²],
eOZT: Existence time in the OZT mesh for each matchmaking relationship [s],
a: Mesh area [km²],
T: Total Time [s], and
n: Number of target ships that generated the OZT in the mesh.

2.4 *Ship position when OZT calculation conditions are satisfied*

When the conditions for calculating the OZT described in Section 2.2 are met, the positions of all the ships that generate OZT in relation to the test ship are examined, and the average number of ships per month is shown on the mesh, where the ships are present. The examination was conducted to determine the locations of the test and target ships, when the conditions were met.

3 ANALYSIS OF SEA AREA AND DATA USED

3.1 *Analysis of sea area*

For the analysed area shown in Figure 5, the estimation has been performed based on the method proposed in this study. The locations of the collisions shown in the figure correspond to the collision cases IV and V which are similar to the collision cases I – III that have been used as references when installing the virtual buoy.

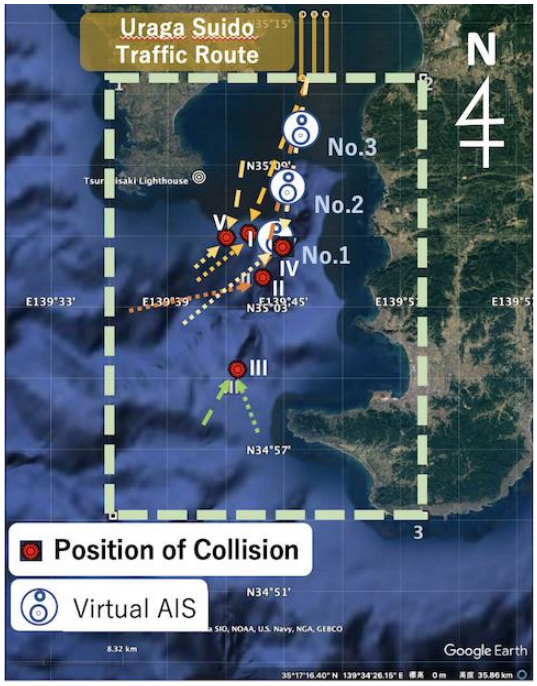

Figure 5. Analysed sea area, positions of the collision, the tracks, and the virtual buoys.

3.2 *Collision cases in the analysis*

Three collision cases (I, II and III) have been discussed and used for verification in the virtual buoy-installation study group [13]. In this study, the locations of two additional collisions (IV and V), involving a north-bound ship and a south-bound ship, are described.

Case I (Collision between south-bound and north-bound ships)

Cargo Ship A was heading south-southwest, and Container Ship B was heading northeast towards Keihin Port, Tokyo, when they collided at 03:10 on 18 March 2014 at the mouth of Tokyo Bay, off the southeast coast of Tsurugisaki, Miura City, Kanagawa Prefecture. When the two ships approached each other, Cargo Ship A turned to the right and Container Ship B turned to the left and continued straight ahead, resulting in a collision between the two ships [7].

Case II (Collision between south-bound and north-bound ships)

Cargo Ship A was proceeding south-southwest, and Cargo Ship B was proceeding northeast, when at approximately 05:18 on 13 April 2006, the bow of Cargo Ship A collided with the port bow of Cargo Ship B, off the east coast of the Miura Peninsula in Kanagawa Prefecture. During the night, visibility was restricted off the east coast of the Miura Peninsula, and owing to inadequate radar coverage of both ships, they inevitably approached each other. Because the speeds of the ships were not reduced to the minimum necessary to maintain their respective courses, the ships could not stop when necessary, and the two vessels collided. The ships were flooded and they eventually sank [10].

Case III (Collision between two north-bound ships)

Cargo Ship A was travelling north-northwest, and Cargo Ship B was travelling north-northeast, when the starboard centre of Cargo Ship A collided with the port bow of Cargo Ship B at approximately 03:49:40, on 16 July 2014, off the northwest coast of Susaki, Tateyama City, Chiba Prefecture. Cargo Ship A suffered a dent with a crack on its starboard hull, and Cargo Ship B suffered a dent with a crack on its port hull. Nonetheless, there were no casualties on either ship. The collision occurred during the night, when the visibility was restricted off the northwest coast of Susaki, despite the fact that Cargo Ship B tried to turn the bow of the ship to 039°. The instructions of the navigator were unclear and Cargo Ship B continued to turn to the right, towards the front of Cargo Ship A. Moreover, the captain of Cargo Ship A might have assumed that Cargo Ship B would eventually turn to the left, and therefore, Cargo Ship A continued to make a small change in direction, and the two vessels collided [8].

Case IV (Collision between south-bound and north-bound ships)

Cargo Ship A was proceeding south and Cargo Ship B was proceeding northward, when at 18:03 on 7 October 1998, at a location 137.5° and 4.8 NM from the Tsurenzaki Lighthouse, the starboard bow of the Cargo Ship A collided with the port bow of the Cargo Ship B at an angle of 21° from astern, while continuing its original course at the initial speed [9].

Case V (Collision between south-bound and north-bound ships)

Car Carrier A was heading north, and Container Ship B was heading south, when at 6:10 p.m. on 24 January 2000 at a location 159° and 3.2 NM from Tsurugizaki Lighthouse, they collided. Car Carrier A was heading 336° when the port bow of the Container Ship B collided with the starboard centre of the Car Carrier A at an angle of 40° from astern [11].

3.3 *AIS Data*

AIS data of three months (from October to December 2018) before the installation of the virtual buoy, and three months (from July to September 2019) after the installation of the virtual buoy, were used. In both cases, before use, the AIS data were interpolated to every 30 s. Figures 6 and 7 show the positions of the north-bound and south-bound ships before and after the installation, respectively. The arrows in the figure indicate the general direction of the ship traffic. It can be seen that before the installation of the virtual buoy, both north-bound and south-bound ships were observed in the vicinity of sites I, II, IV and V, where the collision between the north-bound and south-bound ships occurred as detailed in Section 3.2. After the installation of the virtual buoy, the number of north-bound ships in the vicinity of sites I and V, decreased.

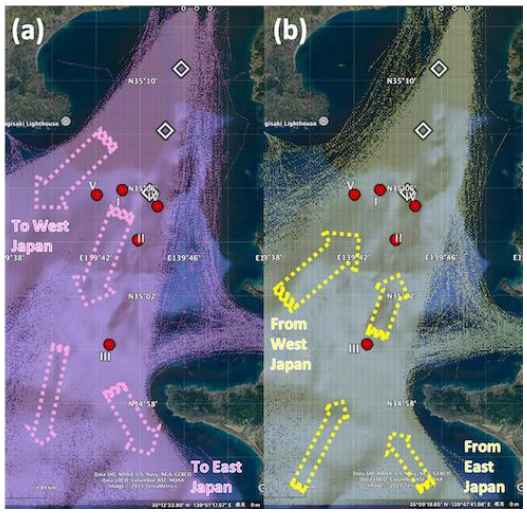

Figure 6. (a) South-bound and (b) north-bound ship positions where one or more ships were observed before the virtual buoy was installed.

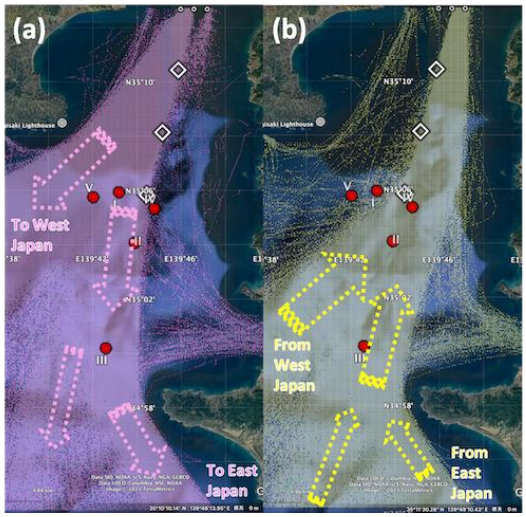

Figure 7. (a) South-bound and (b) north-bound ship positions where one or more ships were observed after the virtual buoy was installed.

4 RESULTS

An absolute evaluation index for the OZT density has not been established yet. Therefore, a comparative evaluation was conducted for the following ship-encounter situations: (1) north-bound test ship and north-bound target ship; (2) north-bound test ship and south-bound target ship; (3) south-bound test ship and north-bound target ship; and, (4) south-bound test ship and south-bound target ship. The evaluation was conducted considering the situation where an OZT exists with one of the ships within ±2° in the direction of the main ship (test ship). Ships with speeds of 6 knots or more and an inter-ship distance of 4 miles or less were analysed using the proposed analysis method. However, tugboats and pilot boats were excluded from the analysis. The maximum value of the colour bar was set such that the sea area where the collision occurred in each matching relationship was close to the middle value and was evaluated comparatively. In this study, ships emerging from the inner part of Tokyo Bay will be referred to as emerging from Uraga Suido, even if they are not navigating through Uraga Suido. Similarly, ships entering Tokyo Bay will be referred to as entering Uraga Suido, even if they are not navigating through Uraga Suido.

4.1 *North-bound test ship and south-bound target ship encounter situation*

This section describes the results of estimating the OZT density and the position of the ship at that time, in relation to the ship emerging from Uraga Suido (north-bound) when the test ship enters Uraga Suido (south-bound). First, Figure 8 (a) shows that before the installation of the virtual buoy, the value of OZT density was relatively high, at approximately 0.015 [times/km^2] or above, in the vicinity of the virtual Buoy 3 (the northernmost buoy), and the value of OZT density decreased as it further moved north. The value of OZT density is approximately 0.01 [times/km^2] in the vicinity of collision sites I, II and IV in this relation. It was also confirmed that the area where the collision occurred did not have the highest OZT density in the comparative evaluation. Figure 8 (b) shows that the spread of the OZT density is smaller than that of Figure 8 (a) before the installation owing to the rectification of the flow of ships emerging from Uraga Suido. From Buoy 3 onwards, the density of OZT in the vicinity of Collision II increases. Figure 9 shows that when the ship entered the Uraga Suido, it intersected with the target ships that generated OZT over a wide area. In the vicinity of the past collision sites I, II, IV and V, it was confirmed that the positions of the test ship and target ships overlapped when the test ship encountered the OZT. Figure 10 (a) shows that the position of the ship, when it encounters the OZT, is concentrated, owing to the rectification of the traffic flow. Between Buoys 1 and 3, it can be confirmed that there are numerous ships experiencing OZTs; however, Figure 10 (b) shows that the positions of the test ship encountering OZTs do not overlap with the positions of target ships that may be causing them. It can also be confirmed that few test ships have encountered the OZT in the vicinity of collision sites I and V in the past. Similarly, in the

vicinity of site IV, no target ships were present. Figure 10 (a) shows the ship encountering OZT, and Figure 10 (b) shows the presence of the target ships in the vicinity of the increased density of OZT on the north side of virtual Buoy 1.

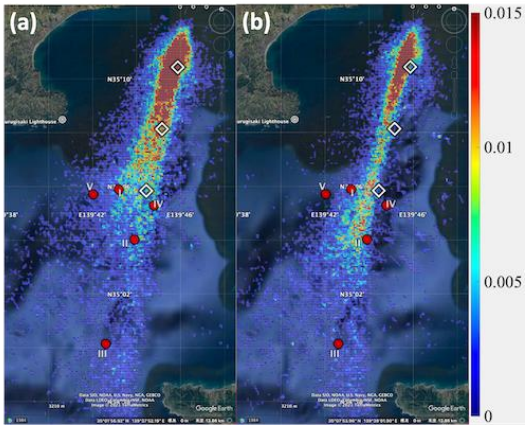

Figure 8. OZT densities (a) before and (b) after the installation of virtual buoy for the south-bound (test) and north-bound (target) ships.

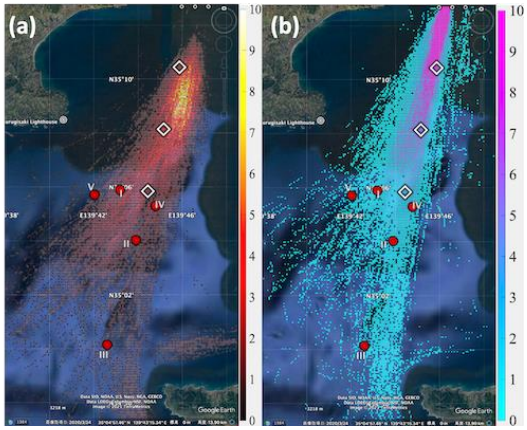

Figure 9. Positions of the (a) test and (b) target ships, when the OZT is calculated before the installation of the virtual buoy.

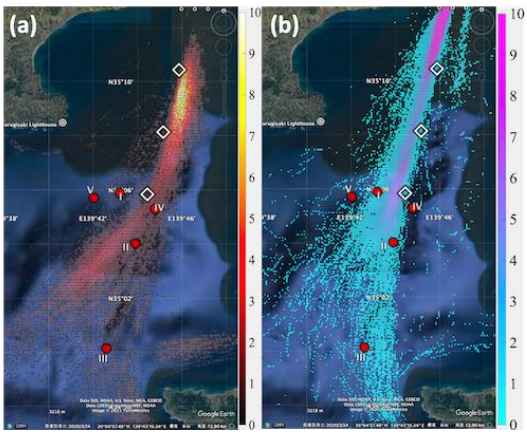

Figure 10. Positions of the (a) test and (b) target ships, when the OZT is calculated after installation of the virtual buoy.

4.2 *South-bound test ship and north-bound target ship encounter situation*

Next, the OZT density and position of the ship that generates it when the test ship leaves the Uraga Suido (south-bound) and the target ship enters the Uraga Suido (north-bound), are discussed. Figure 11 (a) shows that the OZT density is highest at approximately 0.015 [times/km^2] in the vicinity of virtual Buoy 3, and extends to the sea area near Buoy 1 with value of approximately 0.01 [times/km^2]. This trend is similar to that shown in Figure 8. Relatively high values of approximately 0.01 [times/km^2] can also be observed in the vicinity of the past collision sites I, IV and II. Figure 11 (b) shows that the installation of the virtual buoy congests the areas with relatively high OZT density in the path of the ships entering Uraga Suido, and the density is lower than that before the installation. However, the value of OZT density increased to approximately 0.01 [times/km^2] on the south side of Buoy 1, where collision II occurred in the past. Figure 12 (a) and (b) show that when an OZT occurs, there is a possibility that the target ship is approaching from the starboard side of the ship. In particular, in the vicinity of the collision sites I, II and IV, there is a possibility that the test ship is encountering an OZT and that the target ship is approaching from the starboard side. Figure 13 shows that after the installation of the virtual buoy, there are no (or particularly few) ships approaching from the starboard side of the ship, when the ship encounters an OZT from Buoy 1 to 3. However, the number of ships encountering OZT near Buoy 1 increased by approximately 3–5 ships, and the presence of the target ships that may generate OZT south of Buoy 1 was confirmed.

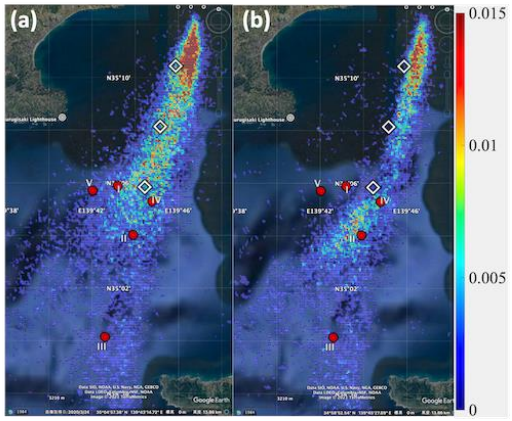

Figure 11. OZT densities (a) before and (b) after the installation of the virtual buoy for the north-bound (test) and south-bound (target) ships.

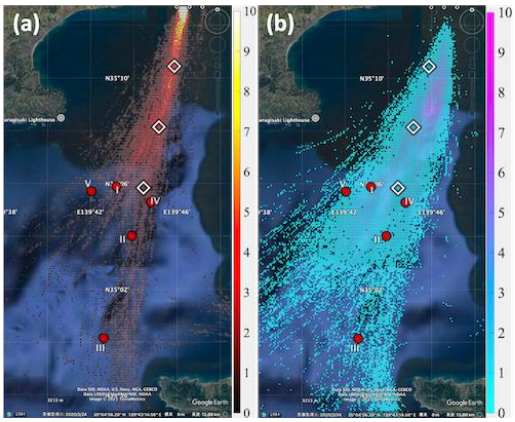

Figure 12. Positions of the (a) test and (b) target ships, when the OZT is calculated before the installation of the virtual buoy.

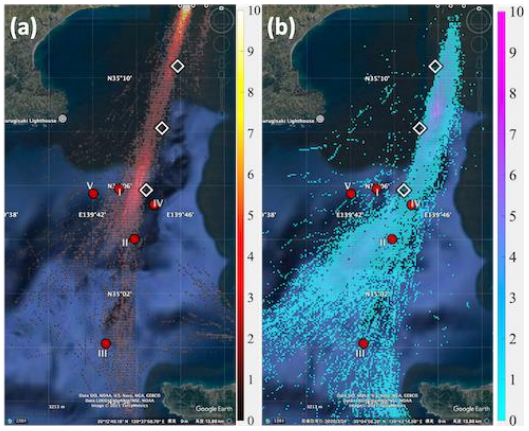

Figure 13. Positions of the (a) test and (b) target ships, when the OZT is calculated after installation of the virtual buoy.

4.3 *North-bound test ship and north-bound target ship encounter situation*

Figure 14 (a) and (b) show that there is no significant change in the OZT density between the test ship and the target ship before and after the installation of the buoy when the ships enter Uraga Suido. The same is true in the vicinity of collision site III, where there is no change in the OZT density of approximately 0.01 [times/km^2]. From the south-side of Buoy 1, the values of 0.015 [times/km^2] or above, are sustained which may be due to the influence of the continuous existence of the OZT owing to the ships navigating in a row for a long time. Figure 15 shows that before the buoy was installed, OZT may have occurred over a wide area when approaching a ship on the starboard side. Furthermore, Figure 16 shows that the buoy has improved the traffic flow for ships that navigate in the same direction and that, when the ship encounters the OZT from Buoy 1 to Uraga Suido, the matching relationship, where the ship approaches the position of the target ship that may be on the right side of the ship, is significantly reduced.

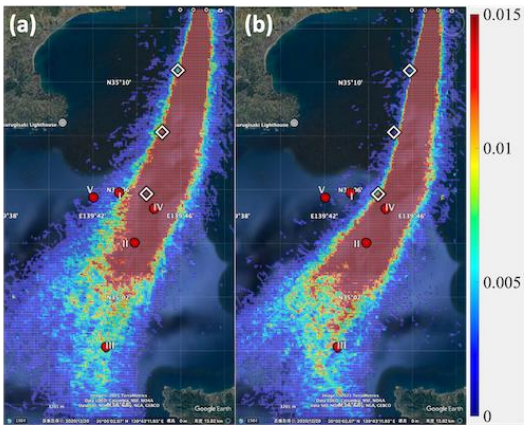

Figure 14. OZT densities (a) before and (b) after the installation of the virtual buoy for the north-bound (test) and north-bound (target) ships.

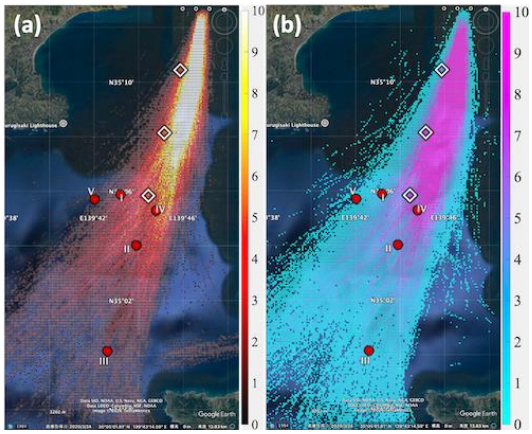

Figure 15. Positions of the (a) test and (b) target ships, when the OZT is calculated before the installation of the virtual buoy.

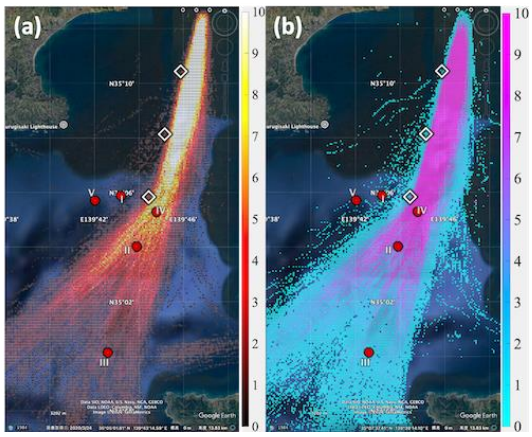

Figure 16. Positions of the (a) test and (b) target ships, when the OZT is calculated after the installation of the virtual buoy.

4.4 *South-bound test ship and south-bound target ship encounter situation*

Figure 17 (a) shows that the OZT density of south-bound ships spreads in a triangular shape from the area where the ships leave Uraga Suido. It can be seen that the density of OZT among the ships leaving Tokyo Bay to Eastern Japan was approximately 0.015 [times/km^2] until Buoy 3. After the installation of the virtual buoy, it can be confirmed that the density of OZT among the ships leaving Tokyo Bay to Eastern Japan increased to approximately 0.015 [times/km^2] along the buoys where approximately 0.01 [times/km^2] before the installation; this trend disappears and the density of OZT decreases after leaving Buoy 1 (the northernmost buoy). In addition to the area along the buoy, the area with a relatively high OZT density decreases. Comparing Figures 18 and 19, the number of ships encountering the OZT along the buoy increased after the installation of the virtual buoy. Comparing Figures 18 (a) and 19 (a), it can be observed that the routes of the ships that are heading for western Japan and those that are heading south are becoming increasingly separated. In case of the OZT density of ships that are not along the buoys heading towards western Japan, the relatively high area decreases.

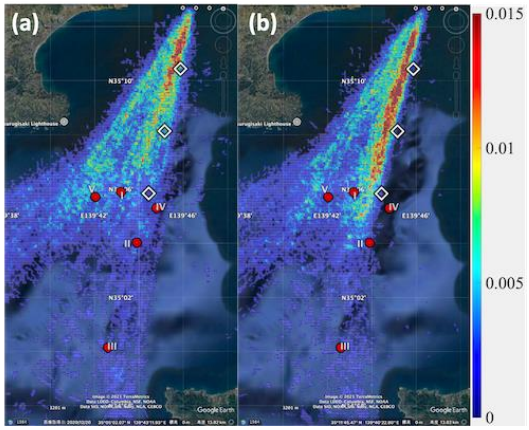

Figure 17. OZT densities (a) before and (b) after the installation of the virtual buoy for the south-bound (test) and south-bound (target) ships.

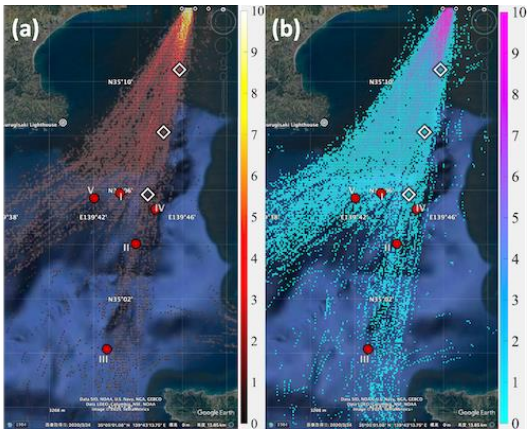

Figure 18. Positions of the (a) test and (b) target ships, when OZT is calculated before the installation of the virtual buoy.

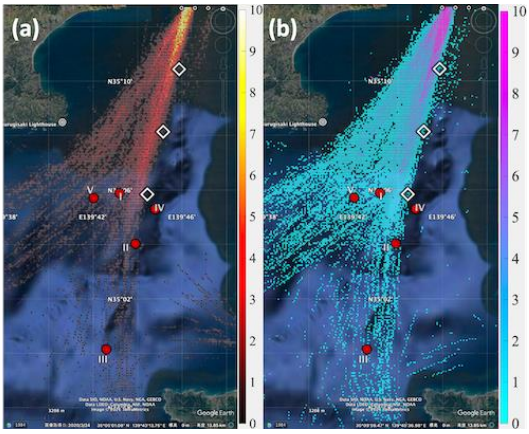

Figure 19. Positions of the (a) test and (b) target ships, when OZT is calculated after the installation of the virtual buoy.

5 DISCUSSION

Considering the relationship between the test ship going towards Uraga Suido and the target ships emerging from Uraga Suido, it can be inferred that at this time, the test ship is the course-keeping vessel and the target ship is obligated to avoid the test ship. Before the installation of the virtual buoy, the test and target ships could not be differentiated in an area with a high OZT density. However, after the installation of the virtual buoy, the test ship could be differentiated from the target ships along the buoy; it is certain that the ships can navigate more safely than before the installation of the virtual buoy, by following the buoy even when OZT exists. However, in the vicinity of the past collision site II, the OZT density increased from approximately 0.005 [times/km^2] to approximately 0.01 [times/km^2], and the positions of the test ship encountering the OZT and its possible target ship overlapped. Therefore, it is difficult to judge whether the installation of virtual buoys improves safety, based on this analysis method. In Figure 10 (b), the position of the south-bound ships shows that the traffic flow of ships leaving the Uraga Suido and continuing southward, is concentrated along the virtual buoy. This makes it easier for the north-bound test ship to predict the position of the target ship, which potentially leads to improved safety.

In the case of a ship leaving Uraga Suido, it is highly probable that the ship will be obligated to take evasive action in relation to a ship entering the channel. Before the installation of the buoy, the position of the ship encountering the OZT overlapped with the position of the target ship at that time, indicating that the ship may have been navigating in a manner that avoided the course of the target ship, to avoid the risk of collision. After the installation of the buoy, ships entering Uraga Suido began to pass to the south of Buoy 1. Therefore, it can be inferred from the decrease in OZT density and the positions of the test and target ships encountering OZTs that the ships are capable of adjusting their course to align with the destination more safely because of the decrease in the number of evasive manoeuvres. However, the OZT density increases from approximately 0.005 [times/km^2] to approximately 0.01 [times/km^2], south of Buoy 1. As mentioned earlier, further analysis is required in this area.

In the case where both the test ship and the target ship were heading towards Uraga Suido, the installation of the virtual buoy significantly reduced the number of ships that are normally from western part of Japan approaching from their starboard side. No significant change in the OZT density or the number of ships was observed in the area of Collision III. However, with the installation of the buoy, it is assumed that ships from the eastern part of Japan navigate along the buoy at an early stage. Therefore, it is implausible that the vessels will navigate through the same course as that in Collision III.

As a result of the installation of the virtual buoy, it is now less probable that ships leaving Uraga Suido and heading southwest and south will encounter ships heading south of Buoy 1 into Uraga Suido. It can be inferred from the decrease in the OZT density that the ships heading southwest can now safely navigate a wider area. It is inferred from the increase in OZT density that the ships sail along the buoy for a long time in the same direction, similar to the ships sailing in the north direction.

Finally, the past collisions did not occur in the area with the highest OZT density; however, in the area with the OZT density of approximately 0.01 [times/km^2], after the installation of the virtual buoy, the area south of Buoy 1 and the area of collision III are the most probable locations for the occurrence of

collision. As mentioned above, the installation of virtual buoys may have improved safety in these waters; however, given the fact that collisions have occurred in waters with an OZT density of approximately 0.01 [times/km^2], it is necessary to navigate these waters more carefully and prevent collisions caused by human error.

6 CONCLUSION

In this study, a virtual buoy installed in Tokyo Bay (by a study committee [13]), was analysed in terms of collisions based on the OZT before and after installation. The existence of OZTs within ±2° in the bow direction was considered a hazard, and all occurrences of OZTs encountered by the ship at that time were included in the analysis. The OZT model was changed from an SD model to an SD3 model, and the OZT was converted to be viewed horizontally from the perspective of the ship. The estimated OZT was used to calculate the OZT density. The positional relationship between the test ship and the target ship in the OZT was used in the analysis. The estimated OZT was used to calculate the OZT density, and the positional relationship between the test ship and the target ship, during the calculation of the OZT, was used in the analysis. It was found that the OZT density was approximately 0.01 [times/km^2] in the places where collisions had occurred in the past. It was confirmed that the installation of virtual buoys reduced the risk of collisions in the locations where collisions had occurred in the past. It was also found that the buoys facilitated in organising the flow of marine traffic, making it easier to predict the movement of ships. Three new passages were created on the south side of virtual Buoy 1, two from south-east and south direction to Uraga Suido, and a third from Buoy 1 to the south. After the installation of the buoy, the OZT density in this area increased from approximately 0.005 [times/km^2] to approximately 0.01 [times/km^2], which is the density observed around past collision sites before the installation of virtual buoys, suggesting that a more detailed analysis is needed in this area. Since there are few analyses that use the location of ship collisions, the results of the OZT density estimation were limited to analysing the changes using the locations where collisions occurred in the past as indicators. However, we were able to demonstrate that the places where ships collide are not necessarily the most congested areas and not the places with the highest OZT density. In the future, if we can develop an absolute index using OZT density, we will be able to make quantitative evaluations and contribute to the reduction of ship collisions.

ACKNOWLEDGEMENT

The authors would like to express their sincere gratitude to the Japan Coast Guard, who provided the AIS data used in this study. This work was supported by JSPS KAKENHI (Grant Number: JP18K13960).

REFERENCES

1. Fukuda, G., Shoji, R.: Development of Analytical Method for Finding the High Risk Collision Areas. TransNav, the International Journal on Marine Navigation and Safety of Sea Transportation. 11, 3, 531–536 (2017). https://doi.org/10.12716/1001.11.03.20.
2. Fukuda, G., Shoji, R.: Estimating Collision Course Area Using OZT in Offshore Refugee Outside the Port. The Journal of Japan Institute of Navigation. 135, 129–134 (2016). https://doi.org/10.9749/jin.135.129.
3. Fukuda, G., Takashima, K.: Analyzing the marine traffic condition for estimating the high risk areas in the emergency evacuation. In: 2015 International Association of Institutes of Navigation World Congress (IAIN). pp. 1–6 (2015). https://doi.org/10.1109/IAIN.2015.7352245.
4. Imazu, H.: Evaluation Method of Collision Risk by Using True Motion. TransNav, the International Journal on Marine Navigation and Safety of Sea Transportation. 11, 1, 65–70 (2017). https://doi.org/10.12716/1001.11.01.06.
5. Japan Coast Guard: Centralizing Marine Traffic Control in Tokyo Bay, https://www.kaiho.mlit.go.jp/e/Centralizing%20Marine%20Traffic%20Control%20in%20Tokyo%20Bay.html, last accessed 2021/03/11.
6. Japan Coast Guard: New Shipping Route Designation at Tokyo Bay Entrance, https://www.kaiho.mlit.go.jp/03kanku/ichigenka/pdf/kokuji_e.pdf, last accessed 2021/03/11.
7. Japan Transport Safety Board: Ship Accident Investigation Report, https://www.mlit.go.jp/jtsb/ship/rep-acci/2016/MA2016-5-1_2014tk0009.pdf, last accessed 2021/03/12.
8. Japan Transport Safety Board: Ship Accident Investigation Report, https://www.mlit.go.jp/jtsb/ship/rep-acci/2015/MA2015-9-15_2014yh0087.pdf, last accessed 2021/03/12.
9. Marine Accident Inquiry and Safety Investigation Association: Cargo ship Kasho Maru cargo ship Blue Peak collision incident, https://nippon.zaidan.info/seikabutsu/2002/00888/contents/0662.htm, last accessed 2021/03/12.
10. Marine Accident Inquiry and Safety Investigation Association: Cargo ship Tsugaru Maru cargo ship Eastern Challenger collision incident, https://maia.or.jp/wp-content/uploads/pdf/accidents/ ㉜ heisei%20zenki.pdf, last accessed 2021/03/12.
11. Marine Accident Inquiry and Safety Investigation Association: Collision of cargo ship Yongchai with cargo ship Toyo Maru No. 12, https://nippon.zaidan.info/seikabutsu/2002/00889/contents/0032.htm, last accessed 2021/03/12.
12. Nishizaki, C., Kayano, J., Shoji, R., Imazu, H.: Encounter Features of Collision Risk in the West Side Sea Area of Izu Oshima using OZT. The Journal of Japan Institute of Navigation. 139, 48–54 (2018). https://doi.org/10.9749/jin.139.48.
13. Tokyo Wan Association for Marine Safety: Study of marine traffic control measures in the waters at the mouth of Tokyo Bay in 2017, http://www.toukaibou.or.jp/img/file18.pdf, last accessed 2021/03/11.